Reactions of Alpha Particles with Iron-54 and Nickel-58†*

FRANK S. HOUCK‡ AND J. M. MILLER
Chemistry Department, Columbia University, New York, New York, and Chemistry Department, Brookhaven National Laboratory, Upton, New York

(Received February 23, 1961)

The excitation functions for the (α,p), (α,n), (α,pn), $(\alpha,2n)$, $(\alpha,p2n)$, and $(\alpha,p2n)$ reactions of Fe^{54} and the $(\alpha,\alpha'p)$, $(\alpha,\alpha'n)$, $(\alpha,\alpha'pn)$, and $(\alpha,\alpha'2n)$ reactions of Ni^{58} have been determined for alpha-particle energies up to 40 Mev. A large preference for proton emission is observed. At the maxima in the excitation functions, these ratios were obtained: $\sigma(\alpha,p)/\sigma(\alpha,n)=3.1$; $\sigma(\alpha,pn)/\sigma(\alpha,2n)=70$; $\sigma(\alpha,\alpha'p)/\sigma(\alpha,\alpha'n)=6$; $\sigma(\alpha,2pn)/\sigma(\alpha,p2n)=6.3$ (at 40 Mev); and $\sigma(\alpha,\alpha'pn)/\sigma(\alpha,\alpha'2n)=140$ (at 40 Mev). These results are discussed in terms of the compound-nucleus model. A value of $r_0=1.7$ fermis is required to fit the low-energy portion of the observed "total" cross section with total reaction cross section calculated from continuum theory.

INTRODUCTION

STUDIES performed during the past several years of nuclear reactions induced by protons and alpha particles with energies up to a few tens of Mev have often shown significant deviations from the predictions that arise from the classical compound-nucleus model for these reactions.[1] The deviations are most clearly seen in the energy and angular distributions of the charged particles that are emitted. The energy spectrum appears to be distorted in the direction of an excess of high-energy particles, and the angular distribution tends to be peaked in the forward direction rather than being symmetrical about $\pi/2$ in the center-of-mass system. These deviations have prompted the introduction of a direct-interaction mechanism as an alternative to the compound-nucleus picture.[2]

On the other hand, when integral experiments such as the excitation functions for charged particle emission are studied, the results appear to be more consistent with a compound-nucleus picture rather than with one involving a direct interaction. For example, studies of the competition between neutron and proton emission, such as the one to be reported here, often show a very large difference between the probabilities of emission for these two particles. With an Fe^{54} target the (α,p) reaction is about three times as probable as the (α,n) reaction, while at the same bombarding energy the (α,pn) reaction is about seventy times as probable as the $(\alpha,2n)$ reaction. Observations of this sort are difficult to reconcile with a direct-interaction mechanism. They are more easily understood in terms of the compound-nucleus picture when the effects of shell structure and pairing energies upon the spacing between the energy levels in the product nuclei are taken into account. The experiments of Ghoshal[3] and of Sagane[4] in which an excited nucleus Zn^{64}, prepared in three different ways—alpha irradiation, proton irradiation, and photon irradiation—emits relative numbers of protons and neutrons which are independent of its mode of formation again speak persuasively for the importance of the compound-nucleus mechanism. Finally, it should be mentioned that the cross-section ratio for the production of isobaric pairs such as Fe^{52} and Mn^{52} in the irradiation of Cr^{50} with alpha particles up to[5] 40 Mev is nearly the same as that observed in the spallation of elements such as cobalt,[6] zinc,[7] and arsenic[8] with protons of approximately 350–400 Mev. In the latter experiments the relative yields of isobaric products are doubtless governed by an evaporation mechanism.

As part of a study of these phenomena we present here the results of an investigation of the interactions of alpha particles with Fe^{54} and with Ni^{58}. With the Fe^{54} cross sections for the (α,p), (α,n), (α,pn), $(\alpha,2n)$, $(\alpha,3n+p2n)$, and $(\alpha,2pn)$ reactions were determined. With the Ni^{58} cross sections for the $(\alpha,\alpha'p)$, $(\alpha,\alpha'n)$, $(\alpha,\alpha'pn)$, and $(\alpha,\alpha'2n)$ reactions—reactions that might well be expected to proceed at least partly through a direct interaction—were determined.

EXPERIMENTAL PROCEDURES

A. Bombardments

The excitation functions were measured in the external alpha-particle beam from the Brookhaven 60-in. cyclotron by means of the stacked-foil technique. The absolute cross section values were all obtained by monitoring the beam intensity during each bombardment through the Zn^{65} activity produced in copper foils interspersed in the target stack. The Zn^{65} activity was

† Submitted in partial fulfillment of the degree of Doctor of Philosophy at Columbia University.

* Research performed under the auspices of the U. S. Atomic Energy Commission.

‡ Present address: Operations Evaluation Group, Massachusetts Institute of Technology, Cambridge, Massachusetts.

[1] See, for example, R. Eisberg and G. Igo, Phys. Rev. **93**, 1039 (1954).

[2] N. Austern, S. T. Butler, and H. McManus, Phys. Rev. **92**, 350 (1953).

[3] S. N. Ghoshal, Phys. Rev. **80**, 939 (1950).

[4] R. Sagane, Phys. Rev. **85**, 926 (1952).

[5] J. M. Miller, G. Friedlander, and S. Markowitz, Phys. Rev. **98**, 1197A (1955).

[6] E. Belmont and J. M. Miller, Phys. Rev. **95**, 1554 (1954).

[7] W. J. Worthington, Jr., University of California Radiation Laboratory Report UCRL-1672, 1952 (unpublished).

[8] J. B. Cumming, Atomic Energy Commission Report NYO-6141, 1954 (unpublished).

measured after the complete decay of the Ga^{65} also produced in the copper foils during the bombardment. Thus the monitoring cross section was the sum of the cross sections for the reactions $Cu^{63}(\alpha,2n)Ga^{65}$ and $Cu^{63}(\alpha,pn)Zn^{65}$. The absolute cross section for the monitor reaction was measured in a separate run with the internal beam through the use of a calibrated current integrator connected to the target probe.

The external focused beam of the cyclotron used for the bombardments of the iron and nickel targets was defined by a 0.5-in.-diam aperture. All targets used with the external beam were square foils 1.5 cm on a side.

B. Targets

All of the copper targets were prepared from 0.5-mil (about 11 mg/cm^2) foil. The targets in the study of the Ni^{58} reactions were 0.3-mil (average of 6.5 mg/cm^2) natural nickel foil. The target stack consisted of alternating nickel and copper foils.

For the iron bombardments a sample of ferric oxide enriched in Fe^{54} was obtained from the Oak Ridge National Laboratory. To prepare the targets the oxide was dissolved and the iron deposited electrolytically from an ammonium oxalate-oxalic acid electrolyte onto copper disks of 8-cm diam and 0.5 mil in thickness. These copper target backings were used to monitor the beam intensity. Each Fe^{54}-plated target foil was weighed prior to the bombardment. After the bombardment and dissolution of the iron with hydrochloric acid, the residual copper backing was weighed. The weight differences, corrected for the small amounts of copper which were also dissolved, determined the thickness of Fe^{54} in each target. The average thickness of the iron platings was about 1 mg/cm^2 with a mean deviation of 3.7%.

Emission spectrographic analyses of the target materials showed no significant impurities.

C. Chemical Separations

Since as many as four to six reaction products were studied in each of the nickel and iron targets, chemical separation of the products into elemental fractions was necessary.

Following bombardment, each iron target foil was treated with hydrochloric acid in order to dissolve the iron under carefully controlled conditions such that only a small and constant (previously determined) amount of the copper target backing was also dissolved. The hydrochloric acid solutions contained cobalt and nickel carriers along with small amounts of zinc, copper, and gallium holdback carriers.

The iron fraction was initially separated by an isopropyl ether extraction from an $8N$ hydrochloric acid solution that contained a little nitric acid. Reextraction into the aqueous phase, a series of three ferric hydroxide precipitations and dissolutions, and a second isopropyl ether extraction were used to remove contaminants from the iron fraction. Finally, the iron was precipitated as the 8-hydroxyquinolate, filtered onto pre-weighed filter paper disks, and weighed to determine the fraction of purified iron activity recovered. The iron samples were then mounted on aluminum counting cards and covered with cellophane.

The cobalt and nickel activities and carriers that remained in the aqueous phase during the iron extraction were then isolated from each other and from other contaminants by a series of ion exchange separations using an anionic exchange resin, Dowex-1.[9] The purified cobalt and nickel fractions were then precipitated as the sulfides, filtered onto paper disks, and prepared for counting. After the various activities had been measured, chemical analyses were performed to determine the chemical yield of each mounted sample. These chemical yields were determined colorimetrically: the nickel by a dimethylglyoxime procedure and the cobalt with ammonium thiocyanate reagent.

The nickel targets were dissolved in a nitric acid solution containing carrier amounts of cobalt, copper, and zinc, the latter two functioning as holdback carriers. The separation and analysis procedures for the cobalt and nickel fractions were essentially those described above for the iron targets.

Chemical separations were also required for the copper foils used to monitor the iron and nickel bombardments because of the recoil of cobalt and iron activities into the copper. After dissolution in nitric acid, cobalt and iron samples were prepared from these copper targets by procedures similar to those outlined above. The zinc fractions were isolated from contaminating activities by ion exchange techniques. Zinc chemical yields were determined by polarography in an alkaline sulfite solution. Chemical separations were not required for the copper targets used in the direct determination of the monitor reactions.

D. Disintegration Rate Determinations

Standards of Fe^{55}, Co^{56}, Co^{57}, and Zn^{65} activities were prepared and their disintegration rates determined with a large side-window argon-methane-filled proportional counter of measured geometrical efficiency. Corrections included those for (1) absorption of the K_α x rays by the samples, by the Be counter window, and by the air between the sample and the counter window; (2) counter efficiency; (3) L capture; (4) internal conversion; (5) fluorescence yield. Table I shows the values of (1) half-life, (2) fluorescence yield (w_K), (3) K-electron captures per disintegration, and (4) K-conversion electrons per disintegration which were used in correcting the counting rates of the Fe^{55}, Co^{56}, Co^{57}, and Zn^{65} standards.

[9] K. A. Kraus and F. Nelson, *Proceedings of the International Conference on the Peaceful Uses of Atomic Energy*, 1955 (United Nations, New York, 1956), Vol. 1, p. 113.

The amounts of Fe^{55} activity in the various iron samples were determined by direct comparison of the samples and standard using the x-ray counter.

The Co^{56} activities were obtained by measuring the samples relative to the standard with a NaI scintillation counter. The scintillation counting equipment included a single-channel pulse-height analyzer which permitted the determination of Co^{56} activity in the presence of both Co^{57} and Co^{58}. Similarly, Co^{57} activities were determined relative to that of the Co^{57} standard with the scintillation counter after subtracting the contribution to the observed activity due to Co^{56} and Co^{58}.

The disintegration rates of Ni^{56} and of Ni^{57} were both obtained indirectly by allowing these activities to decay and then measuring their respective daughter activities, Co^{56} and Co^{57}, in the manner previously indicated.

The counting rates of Zn^{65} activity in those zinc samples which were separated chemically from the copper monitor foils, and hence contained no interfering activities, were determined relative to the Zn^{65} standard with the NaI scintillation counter.

The radioactive products formed in those copper targets which were not subjected to chemical separation were allowed to decay until the only activities remaining, other than Zn^{65}, were Ga^{67} and possibly Cu^{67} and Ni^{63}. By raising the discrimination level of the pulse-height analyzer, all radiations from Cu^{67} and Ni^{63} and all but about 1% of those from Ga^{67} were rejected. The total correction for the counting rates of these Zn^{65} samples due to interfering activities was less than 1%.

The Co^{55} disintegration rates were obtained by means of a calibrated end-window Geiger-Mueller counter. The over-all efficiency of this counting system was determined by means of Na^{22}, Na^{24}, and Co^{60} standards, the disintegration rates of which were determined by coincidence counting. The accuracy of this calibration was checked by measurement of a Ni^{57} sample the disintegration rate of which was subsequently obtained by scintillation counting of the daughter activity. The two disintegration rates so obtained agreed to within the known accuracy of the Ni^{57} branching ratio.[10] Geiger counting was also used to measure half-life values; a half-life of 35.73±0.15 hr was observed for Ni^{57} and that of Co^{55} was measured to be 17.46±0.08 hr. The indicated errors are estimates of the standard deviations based on four or five measurements of each half-life.

TABLE I. Nuclear disintegration data used in computing disintegration rates by x-ray counting.[a]

Isotope	w_K	K-electron captures per disintegration	K-conversion electrons per disintegration	K holes per disintegration	$t_{\frac{1}{2}}$
Fe^{55}	0.26	0.912		0.912	2.94 years
Co^{55}	0.29	0.332		0.332	17.5 hours
Co^{56}	0.29	0.742	$<10^{-3}$	0.742	77.2 days
Co^{57}	0.29	0.916	0.884	1.800	267 days
Zn^{65}	0.39	0.891		0.891	245 days
Ni^{56}					6.4 days
Ni^{57}					35.7 hours

[a] Most of this information was obtained from *Nuclear Level Schemes, A=40—A=92*, compiled by K. Way, R. W. King, C. L. McGinnis, and R. van Lieshout, Atomic Energy Commission Report TID-5300 (U. S. Government Printing Office, Washington, D. C., 1955).

CROSS SECTION RESULTS AND DETERMINATIONS

The excitation function (cross section values) for the combined $Cu^{63}(\alpha,2n)Ga^{65}$ and $Cu^{63}(\alpha,pn)Zn^{65}$ reactions was determined in a bombardment with the internal beam which included a measurement of the integrated beam current. To obtain the incident energy of the internal alpha-particle beam, this excitation function, on a relative cross-section scale, was compared with the same excitation function as measured by Porges.[11] It is estimated that the resulting energy scale is accurate to within about 0.3 Mev at 30 Mev. The total errors in the cross section values are approximately 10%. These errors are predominantly systematic and the same for all of the Zn^{65} samples. The statistical errors due to counting and chemical analyses amount to only 1–2%. Although the shapes of the two excitation functions, shown in Fig. 1, are in good agreement with each other,

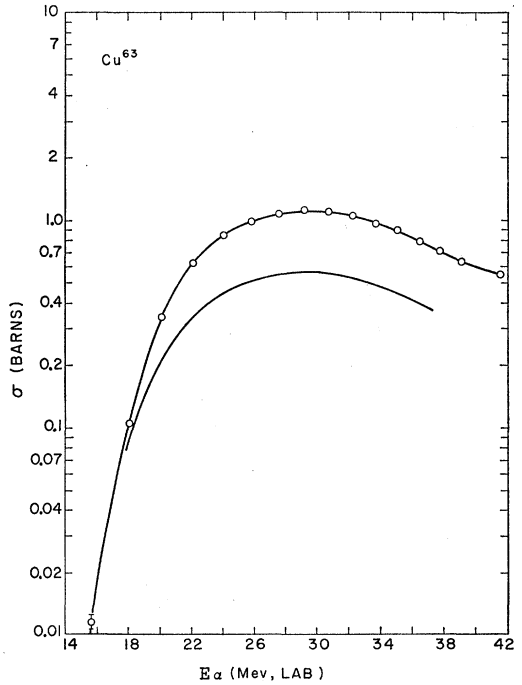

FIG. 1. Energy dependence of the sum of the cross sections for the $Cu^{63}(\alpha,2n)Ga^{65}$ and $Cu^{63}(\alpha,pn)Zn^{65}$ reactions. The solid curve is that determined by Porges[11]; the curve with points is from this work.

[10] D. Strominger, J. M. Hollander, and G. T. Seaborg, Revs. Modern Phys. **30**, 585 (1958).

[11] Karl G. Porges, Phys. Rev. **101**, 225 (1956).

there is an unexplained difference of a factor of 2 in the cross-section scales. In this connection it should be mentioned that the results of Porile and Morrison[12] are in agreement with those of the present experiment.

An excitation function for the production of Zn^{65} in the copper-foil backings and absorbers was determined during each of the iron and nickel bombardments. These curves were then adjusted on both of the coordinates of the $Cu^{63} \rightarrow Zn^{65}$ excitation function to give the alpha-particle energies and the integrated beam current for the monitored reactions. The uncertainty in these energy values is estimated to be no more than 0.4 Mev at 30 Mev.

The excitation functions for the Ni^{58} reactions are presented in Fig. 2. The statistical errors due to the assay of radioactivity and chemical analyses result in a standard deviation for these and the Fe^{54} cross-section values of 1–2% except as otherwise indicated in the figures. In addition, a maximum uncertainty of $\pm 15\%$ due to possible systematic errors is ascribed to both the Ni^{58} and Fe^{54} data.

In measuring these cross sections as for those of all the reactions studied, corrections were made for the recoil of product nuclei from one target foil to the next. The amount of activity transferred by recoil as a result of interaction with 40-Mev alpha particles was about 5% from the 0.5-mil copper foils and up to 40% from the 1–2 mg/cm^2 Fe^{54} target platings. These percentages decrease with decreasing alpha-particle energy.

By virtue of the chemical separation and of the counting procedures, the only interfering activity occurring in the products from Ni^{58} targets is Co^{60} which is produced from Ni^{61} and, in the scintillation counting procedure, is not distinguished from Co^{56}. The assumption that the excitation function of the $Ni^{61}(\alpha,\alpha p)Co^{60}$ reaction is approximately the same as that of the $Ni^{58}(\alpha,\alpha p)Co^{57}$ quite adequately accounts for the low energy (below about 30 Mev) tail observed for the $Ni^{58}(\alpha,\alpha pn)Co^{56}$ reaction. An experimental check for the presence of Co^{60} in a Co^{56} sample resulting from the bombardment of nickel with 40-Mev alpha particles indicated that the contribution of Co^{60} activity to that assigned to Co^{56} would introduce an error of at most about 0.5% in the measured cross section at this energy.

The problem of interfering reactions in the Fe^{54} investigations was largely avoided by the use of enriched Fe^{54}. The results from the Fe^{54} bombardments are shown in Figs. 3, 4, and 5. The very small tail on the $Fe^{54}(\alpha,pn)Co^{56}$ function below 14 Mev can be ascribed to the $Fe^{57}(\alpha,p)Co^{60}$ reaction with the 0.8% of Fe^{57} present in the targets. The other significant interfering reactions occur with Fe^{56} which is present to the extent of 4.4% as determined by proton-activation analysis. The increase of about 10 mb in the cross section for the $Fe^{54}(\alpha,p)Co^{57}$ reaction between 35 and 40 Mev, is due to the $Fe^{56}(\alpha,p2n)Co^{57}$ reaction. If this is corrected for

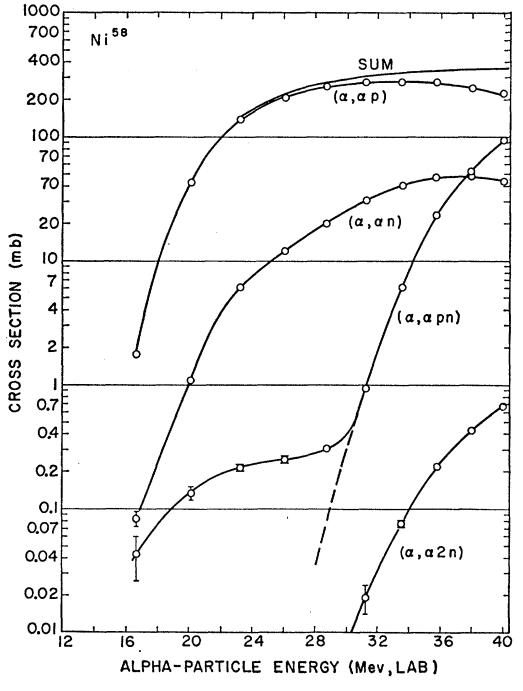

FIG. 2. Excitation functions for the $(\alpha,\alpha' p)$, $(\alpha,\alpha' n)$, $(\alpha,\alpha' pn)$, and $(\alpha,\alpha' 2n)$ reactions of Ni^{58}. The dashed portion of the $(\alpha,\alpha' pn)$ excitation function is the observed excitation function for the production of Co^{56} corrected for the contribution of Co^{60}, formed in the $Ni^{61}(\alpha,\alpha' p)Co^{60}$ reaction, to the Co^{56} counting rate.

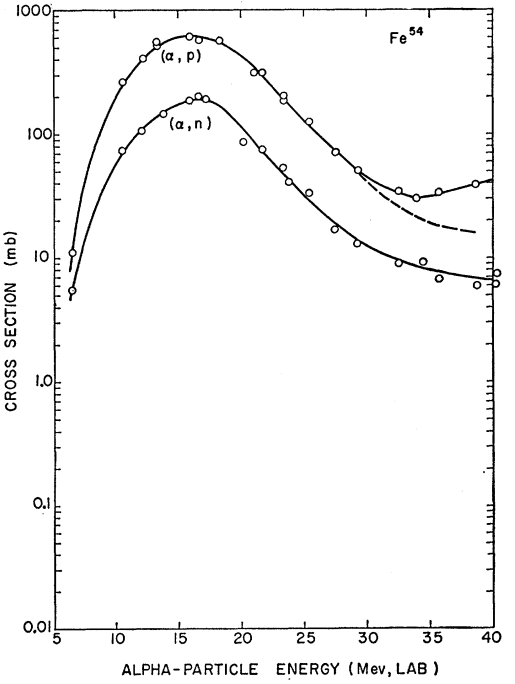

FIG. 3. Excitation functions for the (α,p) and (α,n) reactions of Fe^{54}. The dashed portion of the (α,p) excitation function results from correction of the observed curve section for the contribution of the $(\alpha,p2n)$ reaction with the 4.4% Fe^{56} in the target.

[12] N. T. Porile and D. L. Morrison, Phys. Rev. **116**, 1193 (1959).

from the data of Tanaka *et al.*[13] on the $Fe^{56}(\alpha,p2n)Co^{57}$ reaction, then the cross section of the $Fe^{54}(\alpha,p)Co^{57}$ reaction at high energies is given by the dotted curve in Fig. 3. An upper limit on the contribution of the $Fe^{56}(\alpha,pn)Co^{58}$ reaction to the observed cross section of the $Fe^{54}(\alpha,pn)Co^{56}$ reaction is estimated to be about 5%; a value for this correction of 4.0% was applied to the data.

DISCUSSION

Total Reaction Cross Section

The dependence upon energy of the sum of the measured cross sections for the reactions of alpha particles with iron-54 is displayed in Fig. 6. The sum of the measured cross sections up to alpha-particle energies of approximately 15 Mev should be a good estimate of the total reaction cross section since it is unlikely that any reactions will compete seriously with the (α,p) and (α,n) reactions (the cross section for the (α,γ) reaction is probably less than one millibarn, that for the (α,α') should not affect this part of the curve significantly), both of which were measured. A comparison of the sum curve up to 15 Mev with calculations of the reaction cross section based upon the continuum theory[14] and upon the optical model calculations of Igo[15] leads to a continuum-theory radius parameter (r_0) of between 1.65 and 1.70 f, and indicates a disagreement with the complex potential used by Igo. Although the poor energy resolution at the low-energy end of the excitation functions reported here diminish their usefulness as measurements of a reaction cross section, correction for the energy spread in the beam caused by straggling would move the experimental points to higher energies because the reaction cross section increases more rapidly than the first power of the alpha-particle

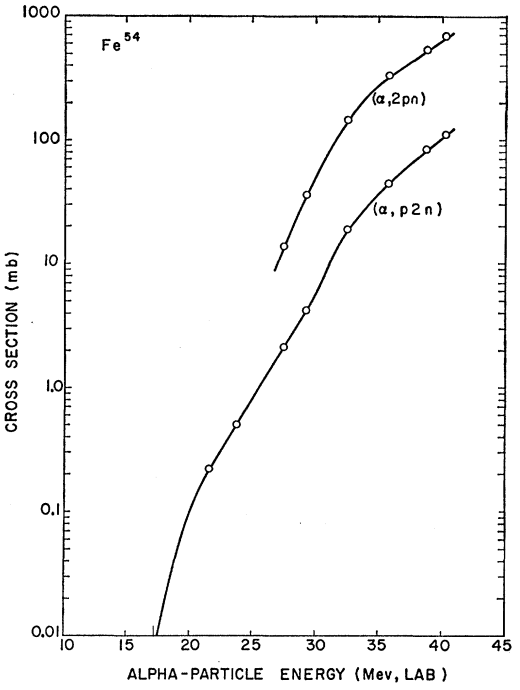

FIG. 5. Excitation functions for the $(\alpha,2pn)$ and $(\alpha,p2n)$ reactions of Fe^{54}.

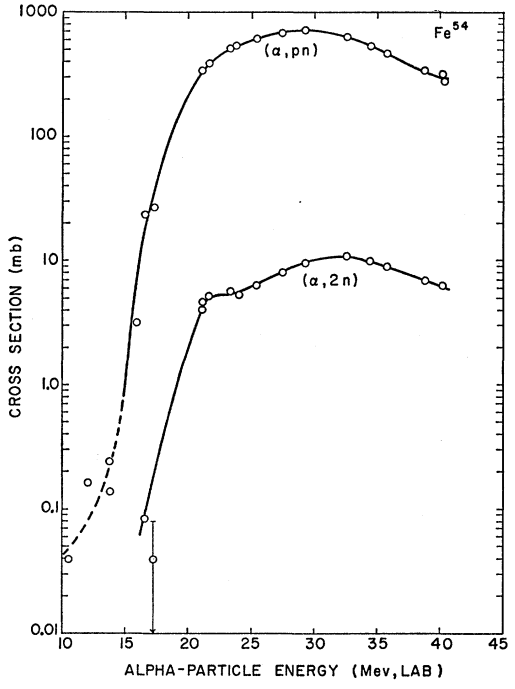

FIG. 4. Excitation functions for the (α,pn) and $(\alpha,2n)$ reactions of Fe^{54}.

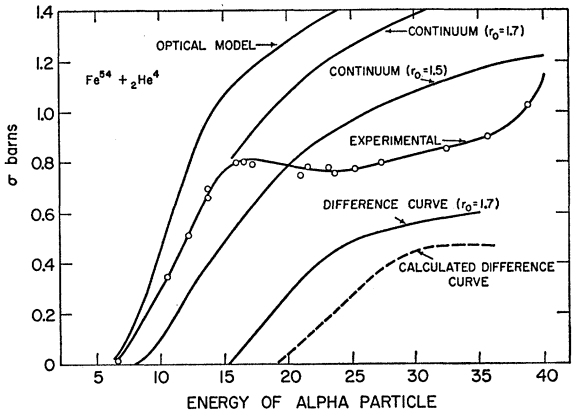

FIG. 6. Sum of measured cross sections compared with reaction cross sections computed from the optical model and from continuum theory. The difference curve is the difference between the experimental curve and that predicted by the continuum theory with $r_0=1.7\times10^{-13}$ cm; the calculated difference curve (the dashed curve) is from reference 17.

[13] S. Tanaka, M. Furukawa, S. Iwata, M. Yagi, H. Amano, and T. Mikumo, J. Phys. Soc. Japan **15**, 2125 (1960) and J. Phys. Soc. Japan **15**, 1547 (1960).
[14] M. M. Shapiro, Phys. Rev. **90**, 171 (1953).
[15] G. Igo, Phys. Rev. **115**, 1665 (1959).

energy and thus make the optical model calculation even further divergent from the experimental values.

The dip in the experimental curve as well as its deviation from the computed one at alpha-particle energies above approximately 15 Mev indicate that there must be several undetected reactions which occur with significant cross sections (see the difference curve in Fig. 6); the obvious candidates are the $(\alpha,2p)$ and the $(\alpha,\alpha'\cdots)$ reactions. Although these are both reactions which have often been assumed to be of negligible importance because of Coulomb barrier considerations, the observations presented here, which show that the (α,pn) reaction is about two orders of magnitude more probable than the $(\alpha,2n)$ reaction and that the $(\alpha,\alpha'\cdots)$ reactions can occur with cross sections of hundreds of millibarns with nickel-58 targets, give strong support to the explanation suggested above.

Qualitative Remarks

The shapes of the individual excitation functions for the reactions of alpha particles with iron-54 nuclei are typical of those expected if the reactions proceeded through the formation of a compound system with subsequent decay governed by the consequences of the usual statistical assumptions. Thus these data, except, perhaps, for the high-energy part of the (α,p) and of the (α,n) reactions, do not seem to require the introduction of noncompound processes for their interpretations.

The most striking feature of these reactions is the impressive preponderance of proton emission over neutron emission, a point that is demonstrated in Figs. 7 and 8 where ratios of cross sections are plotted as a function of alpha-particle energy. The significant probability for proton emission that has been observed previously in *proton* induced reactions[16] has led to the suggestion that the proton emission was to be somehow connected with non-compound processes and should, therefore, occur most markedly in proton induced reactions. The data presented here show clearly that there is no need to invoke these special non-compound processes for proton induced reactions merely because of the significant reemission of protons; the preponderance of proton emission observed in these alpha-induced reactions is greater than that observed in any proton induced reactions that have been investigated. The successful competition of proton emission with neutron emission, which is *only* surprising if *only* the Coulomb barrier to proton emission is considered, has been ascribed to the greater number of final states available to the product of proton emission than to that of neutron emission.

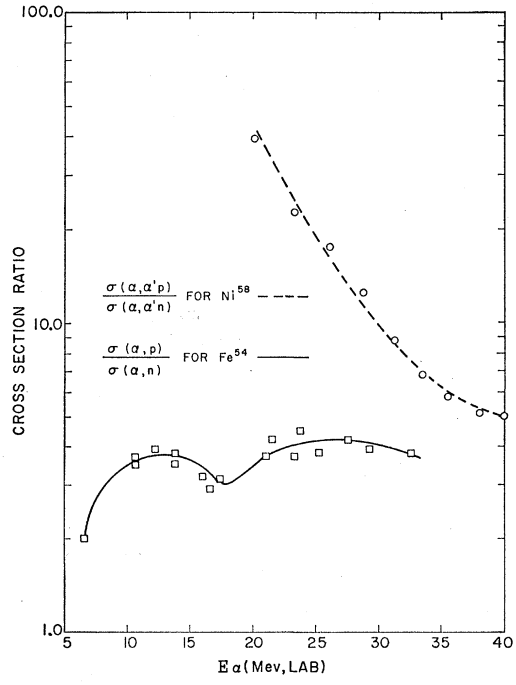

FIG. 7. Comparison of ratio of $(\alpha,\alpha'p)$ and $(\alpha,\alpha'n)$ cross sections of Ni^{58} with that for (α,p) and (α,n) reactions with Fe^{54}.

The "knee" on the low-energy side of the $(\alpha,2n)$ excitation function (see Fig. 4) has also been found by Tanaka *et al.*,[13] and, within the context of the compound-nucleus theory, would arise from a relative sparsity of states within a few Mev of the ground state of Ni^{56} as compared to those of Co^{56}. An attempt at a quantitative formulation of this factor is found in Eqs. (2) and (3). This significant difference in the energy-level structure of Co^{56} and Ni^{56} is also the source of their large difference in formation cross sections. Indeed, above ~35-Mev bombarding energy, the (α,np) reaction is, by calculation,[17] actually more likely than the (α,pn) reaction. Thus, nickel-56 formation remains about two orders of magnitude less likely than cobalt-56 formation, not because of any difficulty in emitting the first neutron, but rather because the second neutron cannot compete at all well with proton emission.

The observation (see Fig. 7) that the ratio of the cross sections for the (α,p) and (α,n) reactions increases with increasing energy after going through a minimum at about 18 Mev is probably to be connected with the onset of the evaporation of two particles. Evidently, in this instance, the (α,n) reaction is depleted earlier and more effectively by the evaporation of a second particle than is the (α,p) reaction. This point will be investigated quantitatively in the next section.

The lower threshold for the (α,p) than for the (α,n) reaction means that the ratio curve in Fig. 7 must turn up toward infinity as the bombarding energy is lowered. This rise and other fine structure that may exist in the ratio curve at low bombarding energies were not observable in this experiment because of a combination

[16] See, for example, Bernard L. Cohen, Phys. Rev. **108**, 768 (1957).

[17] Personal communication from G. Friedlander of unpublished results of calculation described in reference 18.

of two factors: the poor energy resolution of the beam at the low-energy end of the stacked-foil target and the rapid decrease of the reaction cross section at low alpha-particle energies.

The $(\alpha,\alpha'\cdots)$ reactions with nickel-58 were investigated to see if these reactions proceeded through the inelastic scattering of the alpha-particle followed by the evaporation of particles from the residual excited nickel-58 nuclei, and, in particular, to see if these excited nickel-58 nuclei behave in the same manner as those formed by the capture of an alpha particle by iron-54. This mechanism is in contrast to one in which the emitted particles are "directly ejected" by the incident alpha particle. A comparison between the ratio of cross sections for the $(\alpha,\alpha'p)$ and $(\alpha,\alpha'n)$ reactions with nickel-58 with that for the (α,p) and (α,n) reactions with iron-54 as is illustrated in Fig. 7, as well as a similar comparison for those reactions involving the emission of two particles from the excited nickel-58 as shown in Fig. 8, suggests that the protons and neutrons emitted in the $(\alpha,\alpha'\cdots)$ reactions are evaporated subsequent to the inelastic alpha-particle scattering. The large values of the cross section ratios for the $(\alpha,\alpha'p)$ and $(\alpha,\alpha'n)$ reactions shown in Fig. 7 as compared to those for the (α,p) and (α,n) reactions indicate that the inelastic scattering of the alpha-particles often leaves the nickel-58 with low excitation energies, so that the dashed curve reflects the behavior of the solid curve below about 6 Mev, a part of the curve that was inaccessible to measurement in this experiment. The ratio curve for the nickel-58 reactions given in Fig. 8 evidently corresponds to the part of the curve for iron-54 reactions which lies between 20 and 24 Mev in the same figure. The rapid increase in the ratio at lower bombarding energies cannot be observed in the nickel-58 reactions for the same reason as in the iron-54 reactions: The cross section becomes vanishingly small because of the overwhelming competition of one-particle evaporation from nickel-58. Whether or not the primary event, the inelastic scattering of the alpha particle, proceeds through compound-nucleus formation is not immediately clear from these results. But it is worthy of mention at this point, that the very broad maxima which are exhibited by both the $(\alpha,\alpha'n)$ and $(\alpha,\alpha'p)$ excitation functions and which might be taken as qualitative evidence for a direct-interaction process, would also exist according to calculation with compound-nucleus theory because of the onset of the $(\alpha,n\alpha')$ and $(\alpha,p\alpha')$ reaction paths at higher energies.[17]

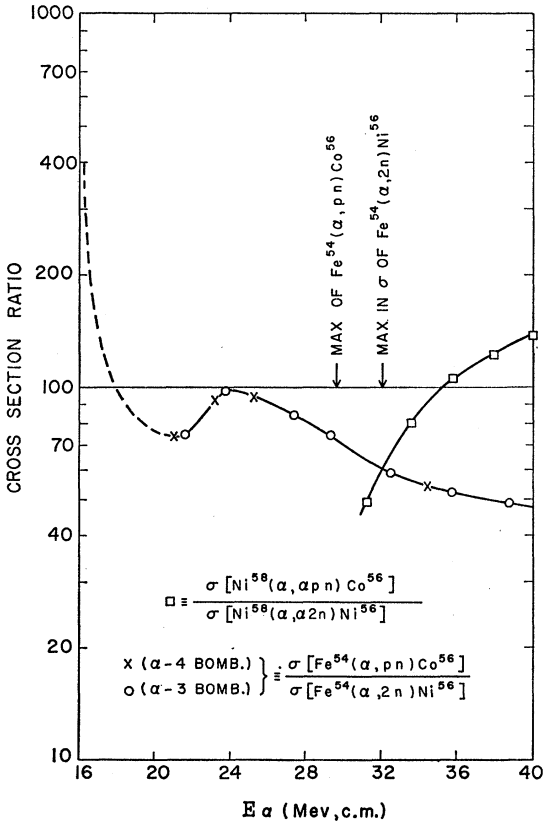

FIG. 8. Comparison of ratio of $(\alpha,\alpha'pn)$ and $(\alpha,\alpha'2n)$ cross sections of Ni^{58} with that for (α,pn) and $(\alpha,2n)$ reactions with Fe^{54}

COMPOUND-NUCLEUS THEORY

The predictions of the compound-nucleus theory for the reactions that were studied in this experiment have been investigated by Dostrovsky, Fraenkel, and Friedlander[18] who employed the Monte Carlo technique for the evaluation of the formalism as described by Weisskopf.[19] Figures 12 and 15 of their paper show that rather good agreement between theory and experiment was obtained. Not presented in their paper, but also calculated, were the cross sections for reactions leading to products that were not observed in this experiment and presumably account for the difference curve in Fig. 6. The computed values are indeed of the same magnitude as the difference curve as is shown by the dashed curve in Fig. 6[17] but, as is often true in their calculation, the calculated curve is displaced toward higher energies. The shift toward higher energies is expected from two features of their calculation. The neglect of energy states below the characteristic level and the approximate treatment of the inverse cross section in charged particle emission will both raise the effective threshold for any given reaction.

The success of the compound-nucleus theory in describing the shapes and magnitudes of excitation functions encourages its use in the analysis of more sensitive quantities such as the ratio curve shown in Fig. 7. This is easily done by integrating the well-known expression for the energy spectrum of a particle emitted

[18] I. Dostrovsky, Z. Fraenkel, and G. Friedlander, Phys. Rev. **116**, 683 (1960).
[19] V. F. Weisskopf, Phys. Rev. **52**, 295 (1937).

from an excited nucleus:

$$I(\epsilon)=(\text{const})M(2I+1)\sigma\epsilon\rho(\epsilon_m-\epsilon), \quad (1)$$

where M is the reduced mass of the system, I is the spin of the emitted particle, σ is the cross section for the inverse process, ϵ is the kinetic energy of the emitted particle in the center-of-mass system, $\rho(\epsilon_m-\epsilon)$ is the density of energy levels of the residual nucleus at an excitation energy $\epsilon_m-\epsilon$, and ϵ_m is the maximum kinetic energy with which the particle may be emitted. In the calculations that follow we shall take

$$\rho(\epsilon_m-\epsilon)=(\text{const})\exp[2a^{\frac{1}{2}}(\epsilon_m-\epsilon-\delta)^{\frac{1}{2}}], \quad \epsilon_m-\epsilon\geqslant\delta, \quad (2)$$

$$\rho(\epsilon_m-\epsilon)=(\text{const}), \quad \epsilon_m-\epsilon\leqslant\delta. \quad (3)$$

These forms take account of the effects of neutron and proton number upon level densities in a manner that is by now standard and also make an effort to consider the energy states below the characteristic level, which is δ Mev above the ground state. The numerical values of δ are taken from the analysis of Dostrovsky *et al.*,[18] as are also the expressions and parameters for particle capture cross sections. These latter expressions are of the form

$$\sigma_n/\sigma_{\text{geom}}=\alpha(1+\beta/\epsilon) \quad \text{for neutron emission,} \quad (4)$$

and

$$\sigma_j/\sigma_{\text{geom}}=(1+C_j)\left(1-\frac{k_jV_j}{\epsilon}\right)$$

$$\text{for charged particles of type } j. \quad (5)$$

The constants α, β, C_j, k_j, as well as the prescription for computing the Coulomb barrier V_j, are given in reference 18. Within this formulation three situations must be distinguished:

(a) $k_jV_j+\delta_j\geqslant\epsilon_m\geqslant k_jV_j$,

(b) $k_jV_j+S_j'\geqslant\epsilon_m\geqslant k_jV_j+\delta_j$,

(c) $\epsilon_m\geqslant k_jV_j+S_j'$,

where the calculation takes those nuclei that result from the emission of particle j and possess an excitation energy above S_j' as being unstable with respect to further particle emission. The quantity S_j' would be expected to be larger than the separation energy of the most loosely bound particle both because of the effects of the Coulomb barrier and competition from photon emission.

The partial width for the emission of *one and only one* charged particle j for each of these situations is given by the integration of (1) with substitutions from (2)–(5):

$$\Gamma_{ja}=(\text{const})M_j(2I_j+1)\sigma_{\text{geom}}(1+C_j)\times[\tfrac{1}{2}(\epsilon_m^2+k_j^2V_j^2)-k_jV_j\epsilon_m],$$

$$\Gamma_{jb}=(\text{const})M_j(2I_j+1)\sigma_{\text{geom}}(1+C_j)\times\left\{\frac{\varphi_1(2a_j^{\frac{1}{2}}(\epsilon_m-k_jV_j-\delta_j)^{\frac{1}{2}})}{8a_j^2}+\delta_j(\epsilon_m-\tfrac{1}{2}\delta_j-k_jV_j)\right\},$$

$$\Gamma_{jc}=(\text{const})M_j(2I_j+1)\sigma_{\text{geom}}(1+C_j)\times\left\{\frac{\epsilon_m-k_jV_j-\delta_j}{2a_j}\varphi_2(2a_j^{\frac{1}{2}}(S_j'-\delta_j)^{\frac{1}{2}})-\frac{1}{8a_j^2}\varphi_3(2a_j^{\frac{1}{2}}(S_j'-\delta_j)^{\frac{1}{2}})+\delta_j(\epsilon_m-\tfrac{1}{2}\delta_j-k_jV_j)\right\}.$$

The functions φ_1, φ_2, and φ_3 are defined as

$$\varphi_1(x)=e^x(2x^2-6x+6)+x^2-6,$$

$$\varphi_2(x)=e^x(x-1)+1,$$

$$\varphi_3(x)=e^x(x^3-3x^2+6x-6)+6.$$

The corresponding expressions for the emission of *one and only one neutron* are:

$$\Gamma_{na}=2(\text{const})M_n\sigma_{\text{geom}}\alpha(\tfrac{1}{2}\epsilon_m^2+\beta\epsilon_m),$$

$$\Gamma_{nb}=2(\text{const})M_n\sigma_{\text{geom}}\alpha\left\{\frac{\varphi_1(2a_n^{\frac{1}{2}}(\epsilon_m-\delta_n)^{\frac{1}{2}})}{8a_n^2}+\frac{\beta}{2a_n}\varphi_2(2a_n^{\frac{1}{2}}(\epsilon_m-\delta_n)^{\frac{1}{2}})+\delta_n(\epsilon_m-\tfrac{1}{2}\delta_n+\beta)\right\},$$

$$\Gamma_{nc}=2(\text{const})M_n\sigma_{\text{geom}}\alpha\left\{\frac{\epsilon_m-\delta_n+\beta}{2a_n}\varphi_2(2a_n^{\frac{1}{2}}(S_n'-\delta_n)^{\frac{1}{2}})-\frac{1}{8a_n^2}\varphi_3(2a_n^{\frac{1}{2}}(S_n'-\delta_n)^{\frac{1}{2}})+\delta_n(\epsilon_m-\tfrac{1}{2}\delta_n+\beta)\right\}.$$

Results calculated from these expressions for the excitation-energy dependence of the ratio of cross sections for the (α,p) and (α,n) reactions with iron-54

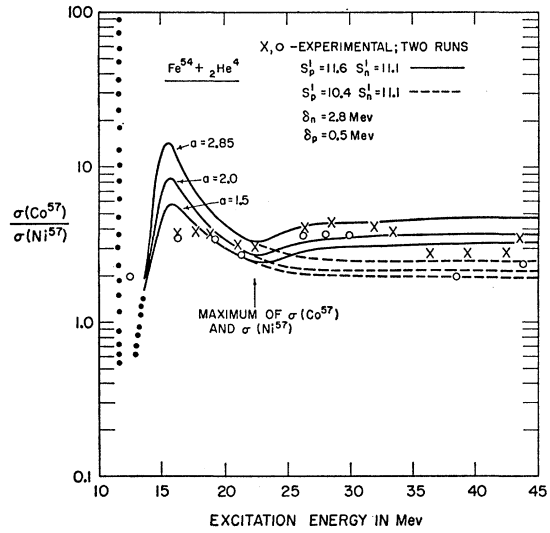

FIG. 9. Comparison between experimental and calculated energy dependence of the ratio of the (α,p) and (α,n) cross section of Fe^{54}.

TABLE II. Table of total binding energies S_p and S_n of the last proton and the last neutron, respectively, for the listed nuclei.[a]

Isotope	S_p (Mev)	S_n (Mev)
Ni^{58b}	7.7	11.7
Ni^{57}	7.6	11.1
Co^{57}	6.2	11.6

[a] *Nuclear Level Schemes, A=40−A=92*, compiled by K. Way, R. W. King, C. L. McGinnis, and R. van Lieshout, Atomic Energy Commission Report TID-5300 (U. S. Government Printing Office, Washington, D. C., 1955).
[b] The value of Q for the formation of the compound nucleus Ni^{58} from an alpha particle and Fe^{54} is 6.39 Mev.

are shown in Fig. 9. The Q values that were used in this computation are given in Table II. The values of δ_n and δ_p were chosen by Dostrovsky *et al.*[18] to reproduce the experimental ratio at the maxima in the excitation functions (excitation energy $U\sim 22$–23 Mev) with $a=2.85$.

A comparison between the calculated and experimental results [corrected for the $Fe^{56}(\alpha,p2n)$ reaction] shows three main points of interest:

(i) The maxima in the calculated curves at about 15.5 Mev of excitation energy are a direct consequence of allowing transition to states below the characteristic level. If no allowance is made for these states, the effective threshold for the (α,n) reaction $(S_n+\delta_n)$ is at 14.5 Mev of excitation energy, which is higher than that of the (α,p) reaction $(S_p+\delta_p+k_pV_p)$. Thus the ratio would approach infinity as U approached 14.5 Mev. While the rather sharp maxima of the curves shown here are the result of the particular form chosen for the level density expression, the general property of going through a maximum depends only upon a rather abrupt change in the rate of increase of level density with excitation energy at some characteristic energy above the ground state. The analysis and compilation by Ericson[20] of existing data on the energy level spectra of various nuclides within several Mev of the ground state show clearly that such abrupt changes do exist.[21] Despite the fact, as was mentioned before, that the energy spread in the beam at the low-energy end of the stacked-foil target would tend to obliterate any detailed structure in the ratio curve, it is evident that the experimental ratios do go through a maximum in roughly the proper region. (The dotted portion of the calculated curve represents an estimate of its behavior in the region where the approximate treatment of charged particle cross sections fails.)

(ii) The quantities S_p' and S_n' are evidently decisive to any attempt to reproduce, within this formalism, the second rise in the ratio above 22.5 Mev. Neither of the two sets of quantities used in this calculation is particularly defensible, but they do illustrate the dependence of the calculation upon S_p' and S_n'. The first set, 11.6 and 11.1 Mev, is the neutron binding energies from Table II; the second set, 10.4 and 11.1, is composed of $S_p+k_pV_p$ for Co^{57} and S_n for Ni^{57}. It is evident that $S_p'>S_n'$ is a necessary condition for a minimum in the computed curves in the vicinity of 22.5-Mev excitation. A more realistic estimate of S_p' and S_n' awaits better information on the competition between photon emission and particle emission at excitation energies near that of the threshold for particle emission.

(iii) As was pointed out by Dostrovsky *et al.*,[18] the calculated (α,p) to (α,n) ratio, particularly near the maxima in their excitation functions, is not very sensitive to a. The agreement between experimental and calculated values in Fig. 9 evidently depends more critically upon S_p' and S_n' than it does upon a.

The ratio $(\Gamma_{nc}+\Gamma_{pc})/(\Gamma_{nb}+\Gamma_{pb})$ represents the sum of the cross sections for the (α,p) and (α,n) reactions divided by the sum of the cross section for all reactions in which either a proton or a neutron is the *first* particle emitted. This is true because the Γ_{jb} give the total width for the emission of particle j. In terms of the experimental data, this quantity may be approximated by

$$(Co^{57}+Ni^{57})/(Co^{57}+Ni^{57}+Co^{56}+Ni^{56}+Fe^{55}+Co^{55}+Ni^{55}).$$

This ratio of experimental quantities is only an upper limit to the proper quantity because it does not include the cross sections for the products of the $(\alpha,2p)$, $(\alpha,n\alpha\cdots)$, and $(\alpha,p\alpha\cdots)$ reactions; but the correction

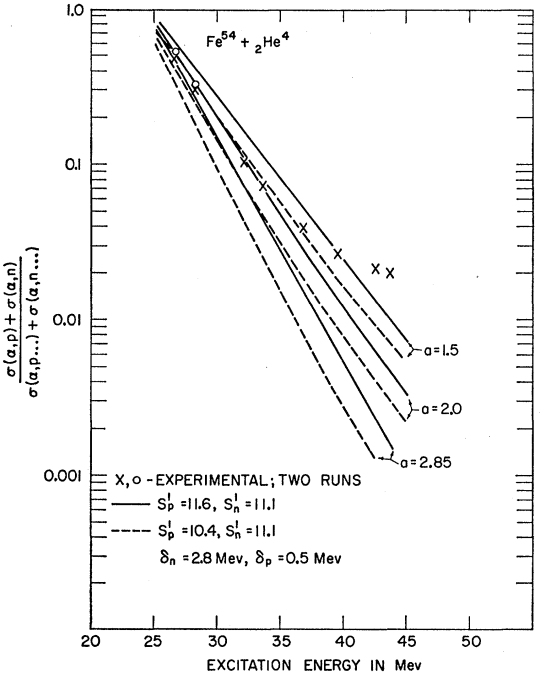

FIG. 10. Comparison between experimental and calculated energy dependence of the fraction of events in which nucleon emission from excited Ni^{58} nuclei is *not* followed by further emission of particles.

[20] T. Ericson, Nuclear Physics **8**, 265 (1958); **11**, 481 (1959).
[21] A. G. W. Cameron, Can. J. Phys. **36**, 1040 (1958).

would surely not be more than 10–20% and is not of qualitative significance. The calculated curves shown in Fig. 10 exhibit appreciable sensitivity to a and to S_p' and S_n'. Comparison between calculation and the experimental points as displayed in Fig. 10, as well as a similar comparison with the results in Fig. 9, leads to a best value of $a\sim 2$ and to the higher value of S_p'.

The divergence between calculation and experiment that sets in above 35 Mev, as exhibited in both Figs. 9 and 10, may reflect the inadequacy of the detailed formalism used in describing the (α,p) and (α,n) reactions at the higher energies. The direction of the divergence in Fig. 10 (the (α,p) and (α,n) cross sections do not diminish rapidly enough at high energies) is qualitatively consistent with a "direct-interaction" approach to this small residual cross section. The results in both Figs. 9 and 10 would be consistent with a direction-interaction contribution to $\sim\frac{3}{4}$ of the (α,p) and (α,n) reactions at the highest energy.

CONCLUSIONS

The comparison between calculated and experimental cross-section ratios over an energy interval in which the cross sections change by as much as a factor of 100 should provide a severe test of the compound-nucleus theory in general as well as a test of the particular form of Eqs. (2) and (3) for the level density. It may thus be concluded that the compound-nucleus model is useful in describing the reactions investigated here and that the simple analytical expression for the dependence of level density upon excitation energy is a reasonable approximation to what is probably a rather complex situation. Since the level densities that are decisive in estimating the cross section for forming particular products are those for the products at an excitation energy below that of the continuum, it is rather surprising that expressions as simple as those in Eqs. (2) and (3) are adequate.

The alternative view of nuclear reactions is one which rejects at least the "statistical assumption" (largely because of the asymmetry in the angular distribution of outgoing particles that has been observed), but goes further in its usual formulation, direct-interaction theory, and rejects the formation of the compound system.[22] To put it differently, the calculation of the cross sections for particular nuclear reactions by compound-nucleus theory depends primarily upon the properties of the possible products of the reactions and only secondarily upon the target nucleus and the incident particle; while in direct-interaction theory, the target nucleus and the incident particle play decisive roles. From the fact that the relative yields of Co^{57} and Ni^{57} are approximately 3 to 4 no matter if they are made by $n+Ni^{58}$,[23] $p+Ni^{58}$,[16,24] $\gamma+Ni^{58}$,[25] or $\alpha+Fe^{54}$ and $\alpha+Ni^{58}$ as in this work, it may be concluded that the characteristics of the product nuclides must be of decisive importance. Thus the successes that have been obtained in interpreting the data within the compound-nucleus theory serve to formalize this more general conclusion.

ACKNOWLEDGMENTS

The authors gratefully acknowledge the cooperation of the operating crew of the 60-in. cyclotron at Brookhaven. We wish to thank Miss F. Ray of Columbia for her assistance in the experiments and Dr. G. Friedlander and Dr. J. R. Grover of Brookhaven for many illuminating conversations. One of us (FSH) wishes to thank the National Science Foundation for the award of a predoctoral fellowship during research.

[22] See, for example, T. Tamura and D. C. Choudhury, Phys. Rev. **113**, 552 (1959).
[23] K. H. Purser and E. W. Titterton, Australian J. Phys. **12**, 103 (1959).
[24] Sheldon Kaufman, Phys. Rev. **117**, 1532 (1960).
[25] J. H. Carver and W. Turchinetz, Proc. Phys. Soc. (London) **73**, 585 (1959).